Desalination and Water Treatment
www.deswater.com

doi: 10.5004/dwt.2021.27652

235 (2021) 107–116
September

Corrosion inhibition of triazines in sulfur-containing oilfield wastewater

Peng Wang[a], Xuefan Gu[a], Quande Wang[a], Jianlong Dong[a], Sanbao Dong[a,b], Jie Zhang[a], Shidong Zhu[a,b], Gang Chen[a,b,*]

[a]*Shaanxi Province Key Laboratory of Environmental Pollution Control and Reservoir Protection Technology of Oilfields, Xi'an Shiyou University, Xi'an Shaanxi 710065, China, Tel. +86-029-88382690; email: gangchen@xsyu.edu.cn (G. Chen)*
[b]*State Key Laboratory of Petroleum Pollution Control, CNPC Research Institute of Safety and Environmental Technology, Beijing 102206, China*

Received 2 April 2021; Accepted 23 July 2021

ABSTRACT

In this study, three kinds of triazines were synthesized via a condensation reaction to inhibit corrosion in oilfield wastewater. The prepared triazines were characterized by infrared spectroscopy and gas chromatography-mass spectrometry, and their performance as eco-friendly corrosion inhibitors in sulfur-containing oilfield wastewater was subsequently evaluated using the weight-loss method and solid-liquid adsorption theory. The results exhibited that triazine II was the most effective corrosion inhibitor in the three and the maximum inhibition efficiency of triazine II (800 mg L^{-1}) can reach 97.66%. The adsorption of the inhibitor was consistent with the assumption of Langmuir adsorption isotherm, the process was spontaneous and chemical adsorption. The mechanism of corrosion inhibition was further explained by desulfurization reaction and coordination bond theory, indicating triazines can be a desulfurizer to synergize their corrosion inhibition in sulfur-containing oilfield wastewater. And their easy adsorption on the steel surface is attributed to nitrogen and oxygen atoms with isolated electron pairs. The above experimental results all indicate that they have the excellent performance to inhibit corrosion, which can be used in oilfield wastewater treatment and will benefit the related research.

Keywords: Triazines; Corrosion inhibition; Adsorption; Oilfield wastewater

1. Introduction

The amount of water resources is used for displacement of reservoir oil in the process of oilfield development, in order to improve oil well production and oil recovery [1,2]. Formation water and injected water are exploited together with crude oil, leading to a large amount of production sewage was produced after oil-water separation on the ground. Noticeably, the amount of high-sulfur wastewater has increased seriously, accompanied by the proportion of high-sulfur crude oil grew in number in the deep crude oil extraction process. Untreated sulfur-containing sewage may cause air pollution and have certain harm to animals and plants when discharged into the environment. In addition, the sulfur-containing oilfield-produced water will also cause corrosion to some extent in the production and injection process, reducing the service life of the machine and production efficiency [3]. In this viewpoint, it is necessary to develop cheap, non-toxic and eco-friendly corrosion inhibitors, particularly indicating the effective desulfurization effect [4,5].

At present, the reported treatment for treating sulfur-containing wastewater mainly include physical methods, chemical methods, biological methods, etc. [6]. The physical and biological treatments generally have a poor effect on the removal of sulfide ions in high-concentration

* Corresponding author.

sulfur-containing sewage. In case of the electrochemical method, the support of the equipment often allowed for the harsh reaction conditions and the long processing time. In comparison, the oxidation method has advantages over deep desulfurization, simple operation and low cost. Essentially, sulfur ions in oilfield wastewater are mainly treated by the oxidation method to oxidize them into harmless elemental sulfur or high-priced oxy salts. On the basis of reducing pollution, the transformation of pollutants to resources can be realized. In recent years, triazine and its derivatives have been widely used as an eco-friendly desulfurized in various industries [7].

Compared with conventional desulfurizers, triazine-based desulfurizers show superiority in low-toxicity, efficiency, biodegradable characteristics [8]. Moreover, the corrosion inhibition of triazine also attracts more interest due to its N-heterocyclic compound with a stable ring structure and sufficient p-electrons. It is generally accepted that organic molecules can be adsorbed on the surface of metal atoms, forming organic films by electrostatic interaction [9–11], thus protecting the metal. Shukla et al. [12] synthesized five kinds of triazine corrosion inhibitors and confirmed that they have excellent corrosion inhibition performance in acid solution, which is related to their active group and electron density. Liu et al. [13] used triazine to solve the problems of blockage and pipeline corrosion caused by sulfur compounds in the transportation of sulfur-containing gas. Kowalczyk [14] proposed that triazine-based desulfurizers have the characteristics of rapid hydrogen sulfide absorption, high sulfur capacity, convenient dosing and low price, which were suitable for offshore oil and gas fields. Castillo et al. [15] conducted performance tests on five triazine-based desulfurizers, and the results showed that injecting the desulfurizer into a mixture containing CO_2 and H_2S can greatly reduce the corrosion rate. In this paper, several kinds of liquid corrosion inhibitors of triazines were synthesized by aldehydes and amines, and their adsorption isotherm, as well as corrosion inhibition performance and mechanism, were further discussed.

2. Experimental

Triazine compounds were prepared by the condensation of aldehydes and amines according to published methods [16–18]. Triazine I, II and III were synthesized by the reaction of formaldehyde with ethylenediamine, ethanolamine and isopropanol amine respectively, the reaction temperature was controlled at 60°C. The molecular structures of synthesized triazines are shown in Fig. 1.

The electrolyte solution was sulfur-containing oilfield wastewater, prepared from analytical grade $Na_2S{\cdot}9H_2O$ and distilled water. And the pH was adjusted to 5 with 0.01 mol L^{-1} hydrochloric acid. The concentration range of inhibitor employed was 200 to 800 ppm in sulfur-containing oilfield wastewater. The corrosion tests were performed on A30 steel sheets (40 mm × 14 mm × 2 mm) with a composition (in wt.%) C: 1.30, Cr: 4.20, Mo: 5.00, V: 3.10, W: 6.40, Co: 8.30 and Fe balance. The tested materials were abraded with a series of emery papers to keep the finish of each surface consistent. The steel sheet was successively soaked in petroleum ether and anhydrous ethanol, and then the surface was dried with a hairdryer.

The structures of synthesized triazines were confirmed by infrared spectroscopy and gas chromatography-mass spectrometry technology. Fourier transform infrared (FTIR) spectra were recorded using the Nicolet 5700 with a 4 cm^{-1} resolution. The sample was evenly applied to the internal mirror and compressed into transparent sheets. Then it was placed on the sample rack for full-wavelength scanning (400–4,000 nm). In gas chromatography-mass spectrometry detection, the mass spectrometry was detected by electric bombardment ionization source (EI), and the gas phase was detected by hydrogen ion flame detector (FID). The analysis conditions of the reaction system with triazine are as follows:

Column: HP-5MS capillary column with the size of 30 × 0.25 mm × 0.25 μm; Column temperature: 50°C, the temperature was raised to 100°C at 10°C min^{-1}, and then to 280°C at 20°C min^{-1} for 5 min; vaporizer temperature: 325°C; detector: hydrogen flame with the temperature set to 250°C; hydrogen: 40 mL min^{-1}; Air: 450 mL min^{-1}; nitrogen: 45 mL min^{-1}.

The weight loss experiments were performed in sulfur-containing oilfield wastewater samples in the absence and presence of various concentrations of triazine corrosion inhibitors. The corrosion inhibition performance was mainly evaluated by calculating uniform corrosion rate and inhibition efficiency. The mass loss is determined after removing from the corrosion solution. The uniform corrosion rates (W_{corr}) have been obtained as suggested in Eq. (1):

$$W_{corr} = \frac{\Delta m}{St} \tag{1}$$

where Δm is the weight loss, mg; S is the exposed area of steel sheet, cm^2; t is the period of immersion of corrosion, h.

The inhibition efficiency (E_w%) was determined by Eq. (2):

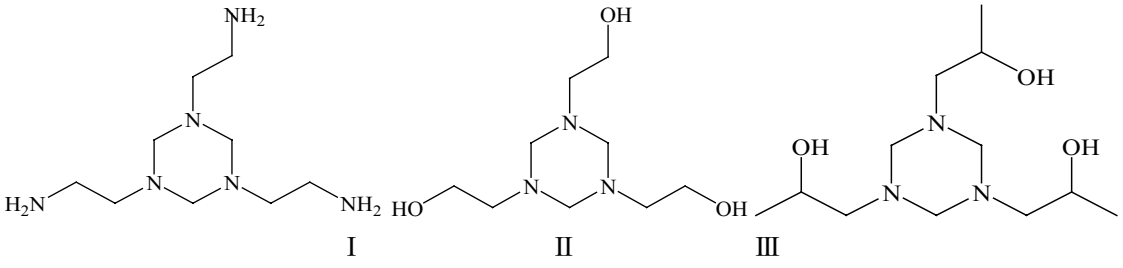

Fig. 1. Structures of synthesized triazine I, II and III.

$$E_w\% = \frac{\Delta m_0 - \Delta m}{\Delta m_0} \times 100 \quad (2)$$

where Δm_0 is the weight loss of the steel sheet in the absence of triazine in the corrosion solution, mg; Δm is the weight loss of the steel sheet in the presence of triazine, mg.

3. Results and discussion

3.1. Fourier transform infrared spectroscopy

FTIR spectra of synthesized triazine I, II and III were shown as Fig. 2. In case of triazine I, symmetrical stretching vibration and asymmetrical stretching vibration bands of amidogen (NH_2) at 3,440 cm^{-1} and methylene (CH_2) at 2,959.3 and 2,820.6 cm^{-1} were observed. It was noticed that the vibration absorption band of variable angle appeared at 1,640 cm^{-1}, CH_2 wagging vibration and CH_2 rocking vibration appears at 1,390; 1,350 and 733 cm^{-1} respectively. On the contrary, the peak at 1,260 cm^{-1} corresponds to the C–N stretching. In addition, extra peaks may appear due to by-products, such as cyanogen and imides, and their intermediate alcohol-amine compound.

In case of triazine II, the strong and wide absorption peak of the O–H bond at 3,485.4 cm^{-1} and O–H out-of-plane bending vibration at 698 cm^{-1} were observed. The absorption peak of the C–O bond appeared at 1,057.8 cm^{-1}, proving that the compound was primary alcohol. The stretching vibration peaks of methylene on the triazine ring and the branched chain were at 2,938.6–28,341.3 cm^{-1}, while the peak at 1,460; 1,350 and 698 cm^{-1} was CH_2 bending vibration, CH_2 wagging vibration and CH_2 rocking vibration. The band at 1,150 cm^{-1} corresponds to the C–N stretching. Furthermore, few significant absorption peaks were observed in the 2,500–2,000 cm^{-1} wavenumber range, indicating triple bonds or cumulative double bonds were not formed in the products. However, compounds containing active hydroxyl groups could dehydrate to form compounds containing double bonds or ether bonds under certain conditions, the peak appeared at 1,640 cm^{-1} was suspected of being C=C stretching vibration, and at 1,150 cm^{-1} could be asymmetrical stretching vibration band of ether bond.

In case of triazine III, a wide absorption peak at 3,392.2 and 682.7 cm^{-1} was detected, indicating stretching vibration of intermolecular hydrogen bond O–H and the O–H out-of-plane bending vibration, respectively. Peaks at 2,952.5 and 2,879.2 cm^{-1} could be ascribed to the asymmetrical stretching vibration and symmetrical stretching vibration bands of CH_3, while those at 1,351.8 and 1,461.8 cm^{-1} could be assigned to the symmetrical and asymmetrical bending vibration of CH_3. The bond at 1,130.1 cm^{-1} was associated with the C–N stretching, then, C–O stretching vibration appeared at 1,072.2 cm^{-1}. Likewise, imines and cyanogen are produced by the action of aldehyde and amino groups, which may bring about the appearance of peaks at 2,150.3 and 1,656.6 cm^{-1}, and the peak at 923.8 cm^{-1} could be the C–O–C stretching vibration. As discussed above, triazine compounds have been synthesized by the reaction of primary amine and formaldehyde, but some by-products were coexistent in this process. Compared with triazine I and triazine III, the synthesized triazine II had fewer impurities.

3.2. Gas chromatography-tandem mass spectrometry

The triazine II with few by-products was further analyzed by gas chromatography-tandem mass spectrometry. And compared with the samples retrieved from the NIST spectrum library, the main peak has appeared. The results showed that the sample contained triazine compounds, solvent (acetonitrile), ethanolamine and a small number of other products or impurities. The results of mass spectrometry are shown in Fig. 3.

3.3. Gravimetric results

The values of corrosion rate and inhibition efficiency of various concentrations of triazines in sulfur-containing oilfield wastewater at 343 K using weight loss technique as summarized in Table 1.

According to Table 1, the corrosion rate of the blank sample reached the highest value. And it can be seen that the severity of the corrosion of steel sheet from Fig. 4. The corrosion inhibition rate reached 68.72% when 400 mg L^{-1} triazine I was added as a corrosion inhibitor, which had a certain degree of corrosion inhibition. With the further increase of concentration, the corrosion inhibition of triazine II was better than that of the other two corrosion inhibitors, and the highest inhibition efficiency was up to 97.66%. It is well known that triazines can significantly inhibit the corrosion of steel sheets. The corrosion rate decreased with the increase of inhibitor concentration, and the inhibition efficiency increased with the increase of inhibitor concentration. The surface of the steel sheet was attached with reddish-brown corrosion products, indicating the presence of Fe_3O_4. Black corrosion products were also attached to the surface of the steel sheet, and the specific phase composition was supposed to be further analyzed by XRD.

The variation curves of corrosion rate and inhibition efficiency with various concentrations of triazines in sulfur-containing oilfield wastewater were drawn according to the data in Table 1. As can be seen from Fig. 5, when the concentration was lower in 200 mg L^{-1}, the corrosion rates of steel sheets treated by triazine I and III were greatly close. With the increase of the concentration of corrosion inhibitor added, the corrosion rate of steel sheet protected by triazine II decreased rapidly and maintained the lowest corrosion rate among the three at any concentration. And in Fig. 6, the inhibition efficiency of triazine II was highest while triazine III was lowest at a low concentration of 200 mg L^{-1}, this may be explained by the hydroxyl groups with large polarity were more prone to metal complex formation at lower concentrations [19,20]. Due to the steric hindrance and the larger molecular weight of triazine III, it was difficult to establish the film formed by adsorption on the metal surface. However, a part of ammonium salt could have been formed by triazine I, resulting in the decrease of the rate of inhibition efficiency. When the inhibitor concentration was more than 400 mg L^{-1}, the growth rate of inhibition efficiency of triazine II decreased slightly, indicating

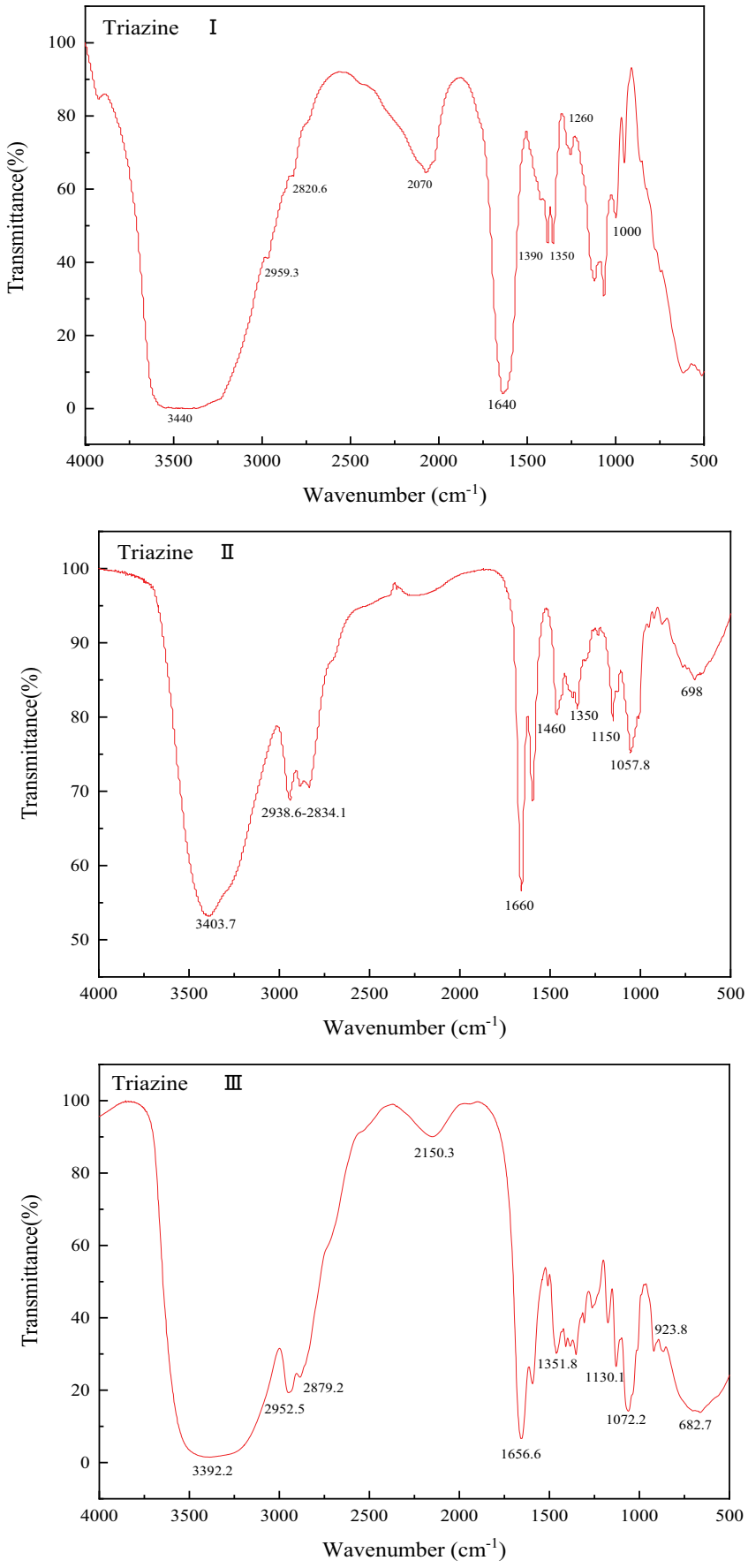

Fig. 2. FTIR spectra of synthesized triazine I, II and III.

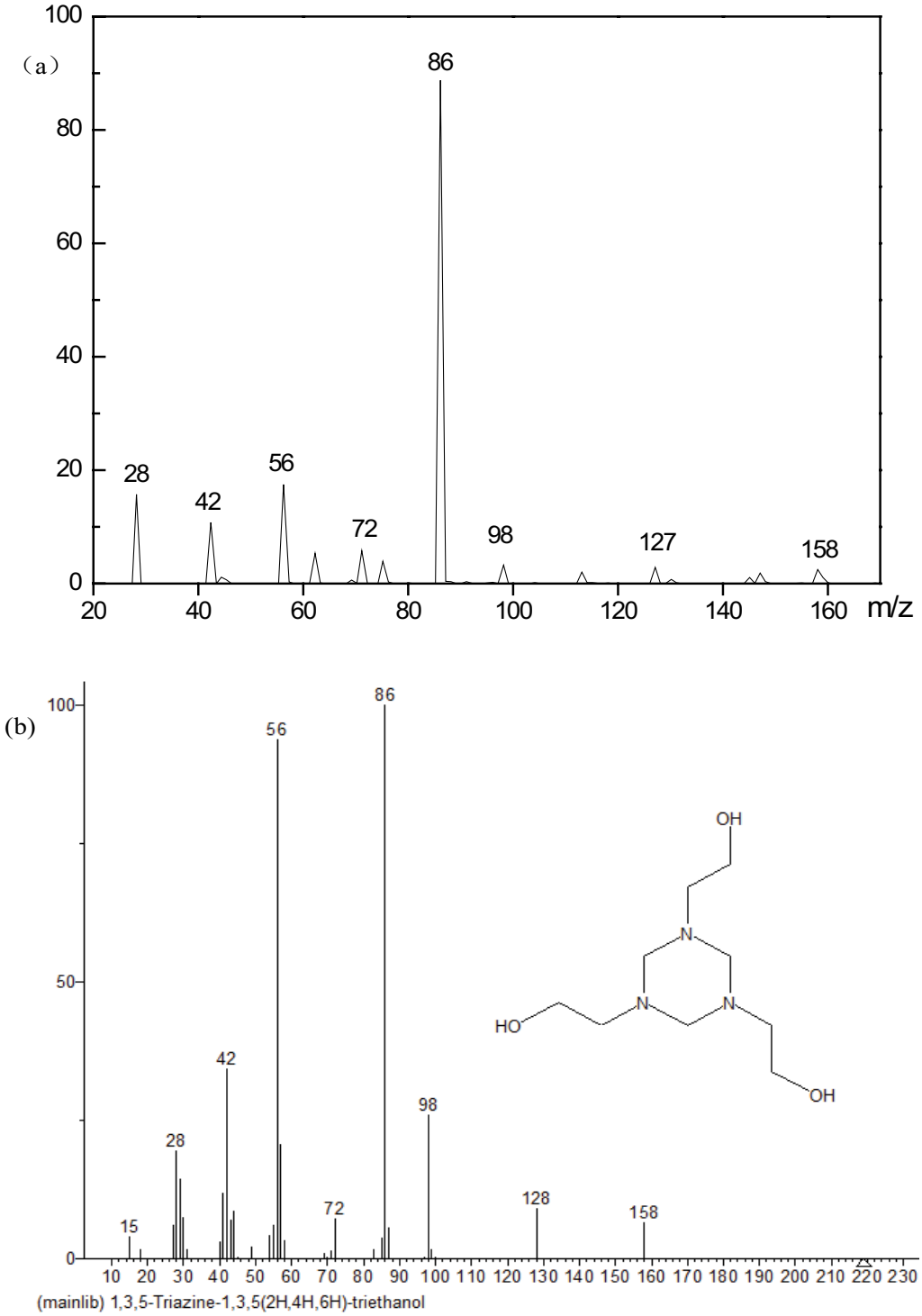

Fig. 3. (a) The mass spectrometry diagram of triazine II and (b) corresponding results of NIST library search.

that the adsorption equilibrium was gradually established, and less reagent was needed to add to achieve full protection action.

3.4. Adsorption isotherm and thermodynamics calculations

According to reports in the literature, the corrosion mechanism of corrosion inhibitors was due to corrosion inhibitor adsorption on the surface of metal [21–23]. The surface coverage (θ) was gradually increased with the increase of concentration of corrosion inhibitor on the steel until the molecular adsorption reached saturation and the coverage tends to 1. The corrosion rate of the steel dropped to the lowest. According to Eq. (3), the surface coverage of corrosion inhibitors at different concentrations was calculated as follow:

Table 1
Valuation of corrosion inhibition of triazines

Inhibitor	Concentrations (mg L^{-1})	Corrosion rates (mg cm^{-2} h^{-1})	Inhibition efficiency (%)
Blank	0	0.21755	/
Triazine I	200	0.11234	48.36130
	400	0.06804	68.72443
	600	0.04080	81.24569
	800	0.01221	94.38750
Triazine II	200	0.09935	54.33234
	400	0.05575	74.37371
	600	0.02940	86.48587
	800	0.00510	97.65571
Triazine III	200	0.11935	45.13905
	400	0.07510	65.47920
	600	0.03585	83.52103
	800	0.01600	92.64537

Fig. 4. Comparison of corrosion inhibition effect of different concentrations of triazines (The first picture on the left showed the uncorroded condition as a comparison).

$$\theta = \frac{W_{corr} - W'_{corr}}{W_{corr}} \quad (3)$$

where W_{corr} is the corrosion rates of A30 steel sheets without triazines, g cm^{-2} h^{-1}; W'_{corr} is the corrosion rate of steel sheets with triazines, g cm^{-2} h^{-1}.

The Langmuir adsorption isotherm assumes the adsorption of organic molecules as a monolayer over the metallic surface without any interaction with other molecules adsorbed [24]. The surface coverage (θ) was related to inhibitor concentration (*C*), which can be evaluated using Eq. (4):

$$\frac{c}{\theta} = \frac{1}{K_{ads}} + C \quad (4)$$

where K_{ads} is the equilibrium adsorption constant of the adsorption process; *f* is the slope of the standard curve.

As can be seen from Fig. 7, three correlated straight lines were obtained (R^2 close to 1) and triazine II had the best linear correlation, indicating that the adsorption of triazines at the interface of the steel and salt solution conforms to the Langmuir adsorption law. The organic molecules can absorb on the surface of steel and block the active corrosion spots, leading to the corrosion rate was reduced [25].

The thermodynamic parameter of the adsorption process of corrosion inhibitor, the Gibbs free energy of adsorption (Δ*G*), was calculated and studied. The values of adsorption equilibrium constant (K_{ads}) of the inhibitors on the steel immersed in sulfur-containing oilfield wastewater were calculated by the Eq. (4) and were summarized in Table 2, the adsorption equilibrium constant of triazine II was relatively large, indicating that the adsorption capacity was larger

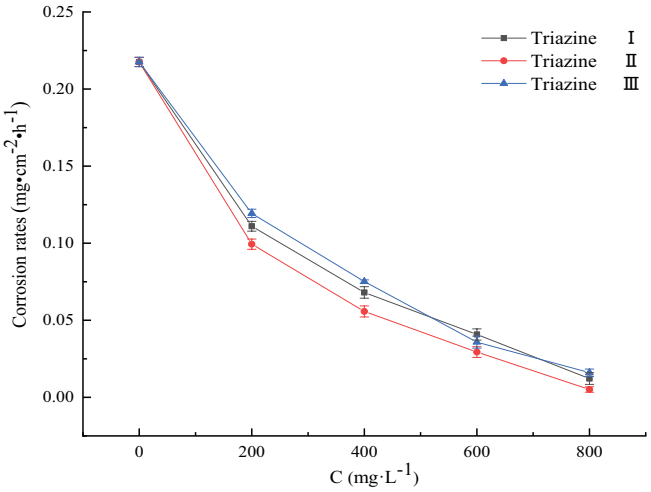

Fig. 5. Variation of corrosion rates in sulfur-containing oilfield wastewater.

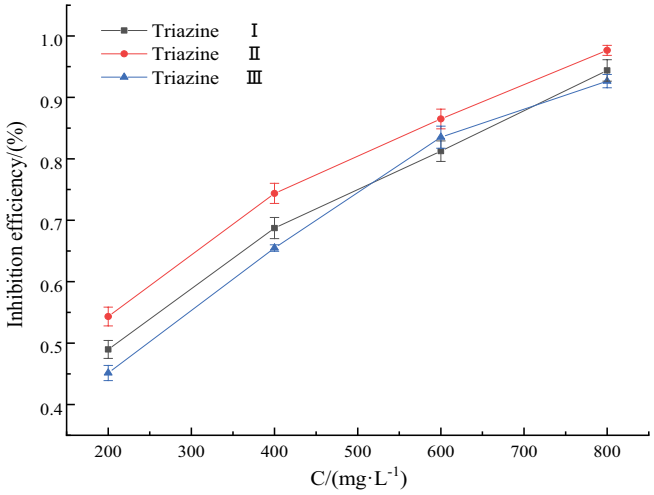

Fig. 6. Variation of inhibition efficiency in sulfur-containing oilfield wastewater.

and conducive to corrosion inhibition, which was consistent with the previous discussion.

The value of adsorption equilibrium constant (K) was related to the Gibbs free energy of adsorption (ΔG):

$$\Delta G_{ads} = -RT\ln\left(55.5K_{ads}\right) \quad (5)$$

where K_{ads} is the equilibrium adsorption constant of the adsorption process; R is the universal gas constant; T is the absolute temperature, K.

The Gibbs free energy of adsorption (ΔG) can be calculated from Eq. (5), which was summarized in Table 2. The results showed that all ΔG values were negative, indicating that the adsorption process was spontaneous. It was reported that if the ΔG absolute values were more than 20 kJ mol^{-1}, the process mainly belonged to chemical adsorption [26,27]. In this sense, triazine II was easier to adsorb spontaneously.

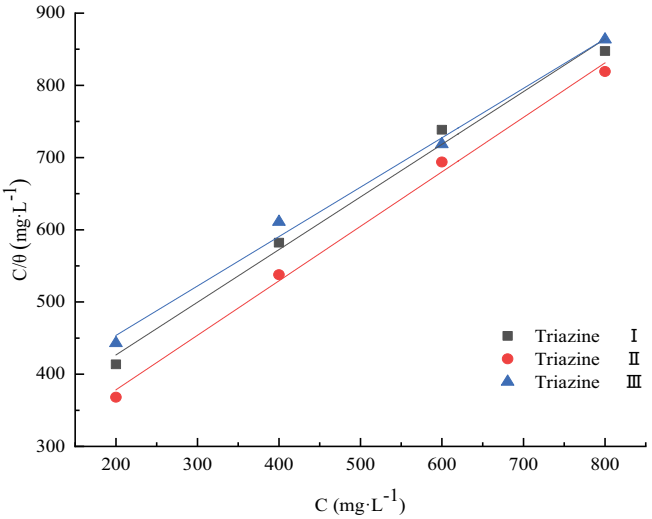

Fig. 7. Langmuir adsorption isotherm plot for the adsorption of triazines on the A30 steel in sulfur-containing oilfield wastewater.

Table 2
Adsorption equilibrium constant (K_{ads}) and ΔG of triazines on the steel surface immersed in sulfur-containing oilfield wastewater

Inhibitor	R^2	f	K_{ads} (L mol^{-1})	ΔG (kJ mol^{-1})
Triazine I	0.99119	0.72926	560.99	–29.50
Triazine II	0.99561	0.75461	726.68	–30.24
Triazine III	0.99355	0.68441	563.92	–29.52

3.5. Inhibition mechanism

The mechanism of corrosion inhibition of prepared triazines in sulfur-containing oilfield wastewater was systematically discussed, based on desulfurization reaction and coordination bond theory. It was generally believed that the active sulfides in the produced oil field water have a strong corrosion effect on the metal equipment [28]. Thus, the corrosion could be distinctly inhibited by reducing sulfur percentage content, owing to the high selectivity to sulfur ions of triazine compounds with the tertiary amine structure [29]. As shown in Fig. 8, the nucleophilic substitution reaction between triazine II and sulfide occurred, producing a new S-containing N-heterocyclic compound. The reaction of 2 molecules of triazine II with 1 molecule of H_2S required lower energy, which was quite easy to occur. As the reaction proceeded, the required energy was higher. In fact, the molar ratio of triazine II and H_2S can reach up to 1:2. It was obvious that the sulfur content in oilfield wastewater was reduced mainly through the reaction of triazine II. In addition, by-product ethanolamine was generated along the reaction process, which also had a certain removal effect on sulfide ions according to literature reports [30]. Above all, triazine II as a desulfurizer could reduce the possibility of corrosion, attributed to its nucleophilic substitution reaction with H_2S (S^{2-}) and the auxiliary removal effect of by-product ethanolamine.

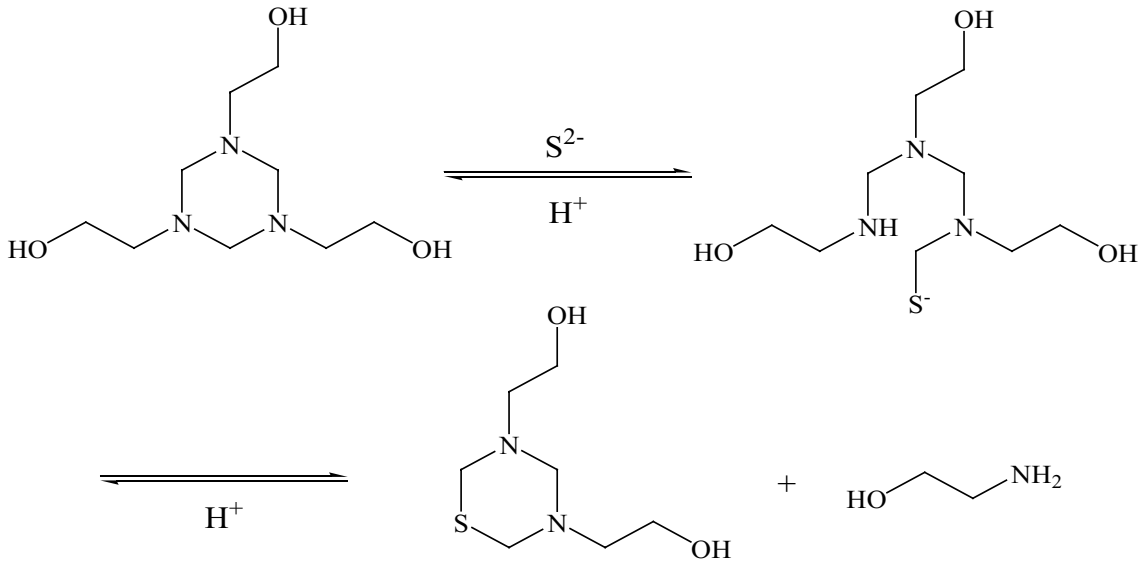

Fig. 8. Nucleophilic substitution of triazine II and hydrogen sulfide.

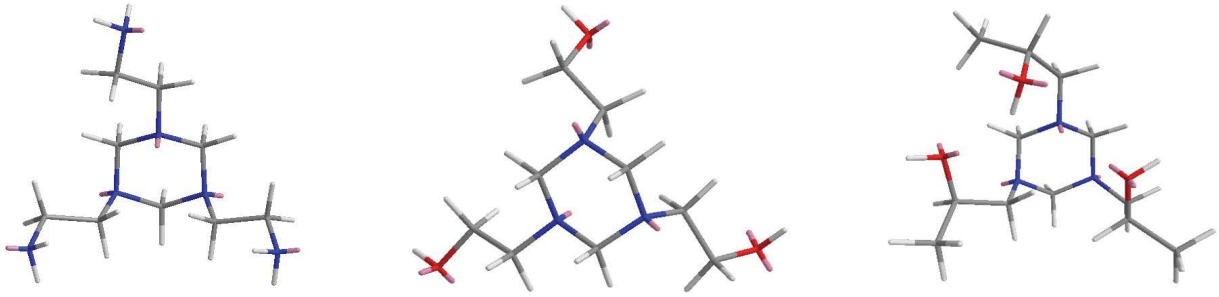

Fig. 9. The steady conformation of triazine I, II and III.

Additionally, it was also reported that the thin layers, formed by corrosion inhibitor molecules and the metal, covered the active sites on the metal surface evenly [31,32], thus inhibiting the corrosion process. In this sense, we further investigated the steady conformation of the aforementioned triazines, using a minimize energy of MM2 in Chem 3D. As shown in Fig. 9, the p-electrons of the hydroxyl groups and amino groups colored in pink sufficiently existed in the steady conformation of triazines, attributed to the presence of electron-rich N and O atoms. The p-d bonds were formatted from the overlap of p-electrons to the 3d vacant orbital of iron atoms, which enhanced the adsorption of the compounds on the metal surface.

In case of triazine II, the schematic illustration of its adsorption on metal is shown in Fig. 10. triazine II can easily absorb on the mild steel surface on the basis of donor-acceptor interactions between p-electrons of the O, N and vacant d orbitals of surface iron. Since the presence of electron-rich O and N of triazine II, a synergistic effect of desulfurization performance and accessible adsorption layer was achieved, significantly improving the inhibition efficiency. Therefore, triazine II is a dual-functional chemical agent with desulfurization and anti-corrosion, which can exert excellent performance in practical applications. In addition, it can avoid adding much more water treatment agents to oilfield wastewater, which is more economical and environmentally friendly compared with the traditional corrosion inhibitor.

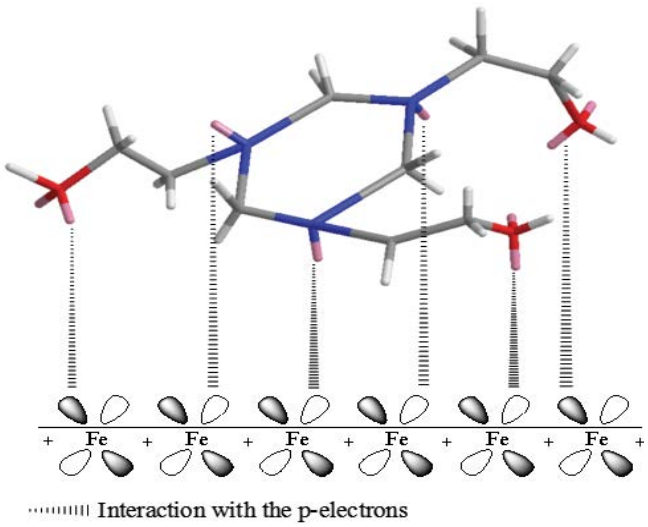

Fig. 10. The absorption of triazine II on the steel surface by coordination.

4. Conclusion

Three kinds of triazines corrosion inhibitors were synthesized with aldehydes and amines. These triazines were characterized by infrared spectroscopy and gas chromatography-mass spectrometry, confirming that the three target inhibitors were all synthesized, and the by-products of triazine II were the least of the three. Their corrosion rate and inhibition efficiency in sulfur-containing oilfield wastewater at different concentrations were investigated by the weight-loss method, the results showed that the inhibition performance of triazines were related to their functional groups and structures. Triazine II had the best inhibition performance, and the maximum inhibition efficiency of triazine II (800 mg L^{-1}) could reach 97.66%. The adsorption process was analyzed by solid–liquid adsorption theory, indicating that it was a spontaneous and chemical process. Furthermore, the probable corrosion inhibition mechanism was explained by the synergistic effect of desulfurization performance and their easy adsorption on the steel surface, which attributed to nitrogen and oxygen atoms with isolated electron pairs. Thus, triazines corrosion inhibitors have great potential for oilfield-produced water containing corrosive ions in the oil and petrochemical industry.

Competing interests

The authors declare that they have no competing interests.

Acknowledgments

This work was financially supported by grants from the National Science Foundation of China (41202214, 51774184), the Youth Innovation Team of Shaanxi University, Shaanxi Provincial Key Research and Development Program (2019ZDLGY06-03) and the Postgraduate Innovation Fund Project of Xi'an Shiyou University (YCS20213154). And we thank the work of the Modern Analysis and Testing Center of Xi`an Shiyou University.

References

[1] L. Wang, Y.M. He, H. Chen, Z. Meng, Z.L. Wang, Experimental investigation of the live oil-water relative permeability and displacement efficiency on Kingfisher waxy oil reservoir, J. Pet. Sci. Eng., 178 (2019) 1029–1043.
[2] W.J. Cao, K. Xie, X.G. Lu, Y.G. Liu, Y.B. Zhang, Effect of profile-control oil-displacement agent on increasing oil recovery and its mechanism, Fuel, 237 (2019) 1151–1160.
[3] H.W. Liu, T.Y. Gu, Y.L. Lv, M. Asif, F.P. Xiong, G.A. Zhang, H.F. Liu, Corrosion inhibition and anti-bacterial efficacy of benzalkonium chloride in artificial CO_2-saturated oilfield produced water, Corros. Sci., 117 (2017) 24–34.
[4] G. Chen, X.Q. Hou, Q.L. Gao, L. Zhang, J. Zhang, J.R. Zhao, Research on Diospyros Kaki L.f leaf extracts as green and eco-friendly corrosion and oil field microorganism inhibitors, Res. Chem. Intermed., 41 (2017) 83–92.
[5] G. Chen, M. Zhang, M. Pang, X.Q. Hou, H.J. Su, J. Zhang, X.J. Hao, Extracts of *Punica granatum* Linne husk as green and eco-friendly corrosion inhibitors for mild steel in oil fields, Res. Chem. Intermed., 39 (2013) 3545–3552.
[6] T.A. Nguyen, R.S. Juang, Treatment of waters and wastewaters containing sulfur dyes: a review, Chem. Eng. J., 219 (2013) 109–117.
[7] S.H. Yoo, Y.W. Kim, K. Chung, N.K. Kim, J.S. Kim, Corrosion inhibition properties of triazine derivatives containing carboxylic acid and amine groups in 1.0 M HCl solution, Ind. Eng. Chem. Res., 52 (2013) 10880–10889.
[8] M. Henrik, J. Carina, S. Erik, Triazine-based H_2S scavenging: development of a conceptual model for the understanding of fouling formation, Pet. Sci. Technol., 32 (2014) 2803–2806.
[9] Y. Bai, J. Zhang, S.B. Dong, J.L. Li, R.J. Zhang, C.S. Pu, G. Chen, Effect of anion on the corrosion inhibition of cationic surfactants and a mechanism study, Desal. Water Treat., 188 (2014) 130–139.
[10] J. Lin, Q.N. Liu, J. Zhang, Y. Wu, H. Li, Y. Ma, C.T. Qu, W.Q. Song, G. Chen, Corrosion inhibition and structure-efficiency relationship study of CTAC and CDHAC, Desal. Water Treat., 139 (2019) 1–6.
[11] Y. Wu, H.J. Yu, S.J. Chen, J. Yan, X.F. Gu, Y. Li, G. Chen, Synthesis and application of a benzotriazole Mannich base as effective corrosion inhibitor for N80 steel in high concentrated HCl, J. Chem. Soc. Pak., 38 (2016) 675–678.
[12] S.K. Shukla, A.K. Singh, M.A. Quraishi, Triazines: efficient corrosion inhibitors for mild steel in hydrochloric acid solution, Int. J. Electrochem. Sci., 7 (2012) 3371–3389.
[13] Q. Liu, J. Whittaker, R. Allende-Garcia, A. McIntyre, J. Magyar, K. Tamminga, Corrosion management and cleaning of SAGD produced gas/H_2S scavenger contactor, Corrosion, 2014 (2014) 3808.
[14] B.A. Kowalczyk, A short total synthesis of palonosetron using catalytic hydrogenation, Heterocycles, 43 (1996) 1439–1446.
[15] M. Castillo, Y.S. Avila, R.E. Rodriguez, A. Viloria, Liquid scavengers – their effectiveness and compatibility with downstream processes, Mater. Perform., 39 (2000) 54–58.
[16] A. Majhi, S.S. Kim, S.T. Kadam, Rhodium(III) iodide hydrate catalyzed three-component coupling reaction: synthesis of a-aminonitriles from aldehydes, amines, and trimethylsilyl cyanide, Tetrahedron, 64 (2008) 5509–5514.
[17] A.R. Katritzky, L.H. Xie, G.F. Zhang, M. Griffith, K. Watson, J.S. Kiely, Synthesis of primary amines via nucleophilic addition of organometallic reagents to aldimines on solid support, Tetrahedron Lett., 38 (1997) 7011–7014.
[18] R.E. Quiñones, C.M. Glinkerman, K.C. Zhu, D.L. Boger, Direct synthesis of β-Aminoenals through reaction of 1,2,3-triazine with secondary amines, Org. Lett., 19 (2017) 3568–3571.
[19] Q.N. Liu, M.L. Gao, C.T. Qu, R.J. Zhang, Z.F. Song, J.L. Li, G. Chen, Synthesis and interface activity of cetyltrimethylammonium benzoate, Russ. J. Phys. Chem. B, 14 (2020) 73–80.
[20] Q.N. Liu, M.L. Gao, Y. Zhao, J.L. Li, C.T. Qu, J. Zhang, G. Chen, Synthesis and interfacial activity of a new quaternary ammonium surfactant as an oil/gas field chemical, Tenside, Surfactants, Deterg., 57 (2020) 90–96.
[21] M.L. Gao, J. Zhang, Q.N. Liu, J.L. Li, R.J. Zhang, G. Chen, Effect of the alkyl chain of quaternary a mmonium cationic surfactants on corrosion inhibition in hydrochloric acid solution, C.R. Chim., 22 (2019) 355–362.
[22] K.K. Alaneme, S.J. Olusegun, O.T. Adelowo, Corrosion inhibition and adsorption mechanism studies of *Hunteria umbellata* seed husk extracts on mild steel immersed in acidic solutions, Alexandria Eng. J., 55 (2016) 673–681.
[23] G. Chen, H.J. Su, Y.P. Song, Y. Gao, J. Zhang, X.J. Hao, J.R. Zhao, Synthesis and evaluation of isatin derivatives as high concentrated hydrochloric acid corrosion inhibitors for Q235A steel in oil field, Res. Chem. Intermed., 39 (2013) 3669–3678.
[24] K. Yang, J. Fox, DPF soot as an adsorbent for Cu(II), Cd(II), and Cr(VI) compared with commercial activated carbon, Environ. Sci. Pollut. Res., 25 (2018) 1–16.
[25] M.S. Hong, Y. Park, J.G. Kim, K. Kim, Effect of incorporating MoS_2 in organic coatings on the corrosion resistance of 316L stainless steel in a 3.5% NaCl solution, Coatings, 9 (2019) 45, doi: 10.3390/coatings9010045.
[26] Z. Bekçi, Y. Seki, M.K. Yurdakoç, Equilibrium studies for trimethoprim adsorption on montmorillonite KSF, J. Hazard. Mater., 133 (2006) 233–242.
[27] F.F. Chen, Q.J. Liu, Z.M. Xu, X.W. Sun, Q. Shi, S.Q. Zhao, Adsorption kinetics and thermodynamics of vanadyl etioporphyrin on asphaltene in pentane, Energy Fuels, 27 (2013) 6408–6418.

[28] S.S. Chen., J.G. Wang, Z.G. Wang, Hydrogen sulfide corrosion of metal equipment in oil and gas field, Pet. Drill. Technol., 39 (2011) 32–35.
[29] J.L. Kice, J.D. Campbell, Mechanisms of substitution reactions at sulfinyl sulfur. VII. General base catalysis by a tertiary amine of the hydrolysis of an aryl sulfinyl sulfone, J. Org. Chem., 36 (1971) 2291–2294.
[30] X. Liu, B. Wang, X. Lv, Q. Meng, M. Li, Enhanced removal of hydrogen sulfide using novel nanofluid system composed of deep eutectic solvent and Cu nanoparticles, J. Hazard. Mater., 405 (2020) 124271, doi: 10.1016/j.jhazmat.2020.124271.
[31] X.F. Gu, K. Dong, J. Tian, H. Li, J. Zhang, C.T. Qu, G. Chen, Investigation of modified Ginkgo biloba leaves extract as eco-friendly inhibitor for the corrosion of N80 steel in 5% HCl, Desal. Water Treat., 107 (2008) 118–126.
[32] G. Chen, M. Zhang, J.R. Zhao, R. Zhou, Z.C. Meng, J. Zhang, Investigation of *Ginkgo biloba* leave extracts as corrosion and oil field microorganism inhibitors, Chem. Cent. J., 7 (2008) 83, doi: 10.1186/1752-153X-7-83.